Biol Blood Marrow Transplant 20 (2014) 1493–1500

Biology of Blood and Marrow Transplantation

journal homepage: www.bbmt.org

ASBMT American Society for Blood and Marrow Transplantation

Biology

Endothelial Dysfunction and Altered Mechanical and Structural Properties of Resistance Arteries in a Murine Model of Graft-versus-Host Disease

Peter M. Schmid [1,*], Abdellatif Bouazzaoui [2], Kristina Doser [2], Karin Schmid [2], Petra Hoffmann [2], Josef A. Schroeder [3], Guenter A. Riegger [1], Ernst Holler [2], Dierk H. Endemann [1]

[1] Medical Clinic 2, Cardiology, University Hospital Regensburg, Germany
[2] Medical Clinic 3, Hematology/Oncology, University Hospital Regensburg, Germany
[3] Institute for Pathology, University Hospital Regensburg, Germany

Article history:
Received 24 February 2014
Accepted 1 May 2014

Key Words:
Endothelial dysfunction
Compliance of resistance arteries
Graft-versus-host disease
Endothelial nitric oxide synthase (eNOS)
Inducible nitric oxide synthase (iNOS)

A B S T R A C T

A putative involvement of the vasculature seems to play a critical role in the pathophysiology of graft-versus-host disease (GVHD). We aimed to characterize alterations of mesenteric resistance arteries in GVHD in a fully MHC-mismatched model of BALB/c mice conditioned with total body irradiation that underwent transplantation with bone marrow cells and splenocytes from syngeneic (BALB/c) or allogeneic (C57BL/6) donors. After 4 weeks, animals were sacrificed and mesenteric resistance arteries were studied in a pressurized myograph. The expression of endothelial (eNOS) and inducible nitric oxide (NO)–synthase (iNOS) was quantified and vessel wall ultrastructure was investigated with electron microscopy. The myograph study revealed an endothelial dysfunction in allogeneic-transplant recipients, whereas endothelium-independent vasodilation was similar to syngeneic-transplant recipients or untreated controls. The expression of eNOS was decreased and iNOS increased, possibly contributing to endothelial dysfunction. Additionally, arteries of allogeneic transplant recipients exhibited a geometry-independent increase in vessels strain. For both findings, electron microscopy provided a structural correlate by showing severe damage of the whole vessel wall in allogeneic-transplant recipient animals. Our study provides further data to prove, and is the first to characterize, functional and structural vascular alterations in the early course after allogeneic transplantation directly in an ex vivo setting and, therefore, strongly supports the hypothesis of a vascular form of GVHD.

INTRODUCTION

Allogeneic bone marrow transplantation (BMT) is the only curative therapy for a variety of hematological disorders. In the treatment of malignant diseases, the efficacy of allogeneic BMT relies not only on the preceding high-intensity chemotherapy, but mainly on the response of transplanted immune cells against leukemic cells or the tumor (graft-versus-leukemia/tumor). Unfortunately, this positive immune response is closely correlated with graft-versus-host disease (GVHD), in which the cytotoxic donor T cells affect healthy recipient tissues, causing organ injuries and resulting in high morbidity and mortality. Therefore, GVHD is the main limitation of allogeneic BMT for a broader and safer clinical use [1-3].

The vasculature, and especially the endothelium, seems to play an important role in the development of acute GVHD, as it forms the first frontier between the alloreactive donor cells and the recipient's tissue [4]. Because the early course after BMT is complicated by vascular injury syndromes, such as transplantation-associated microangiopathy, veno-occlusive disease, or the capillary-leak syndrome, and in the later course by atherosclerotic cardiovascular complications, the existence of a vascular form of GVHD is postulated [5-10]. This hypothesis is supported by histological findings in skin samples in acute GVHD [11,12], an increased count of circulating endothelial cells [13], and endothelial cell chimerism after BMT [14]. Furthermore, an increased expression of endothelial adhesion molecules [15-20], as well as elevated serum levels of soluble adhesion molecules [21], are described in GVHD.

However, the incidence of an endothelial dysfunction in the course of clinical GVHD is, up until now, only supported indirectly by serum markers of endothelial function in humans [22-26]. Functional studies, as well as a detailed

Financial disclosure: See Acknowledgments on page 1499.

* Correspondence and reprint requests: Dr. med. Peter M. Schmid, Medical Clinic 2, Franz-Josef-Strauss Allee 11, University Hospital Regensburg, 93042 Regensburg, Germany.
E-mail address: peterm.schmid@ukr.dr (P.M. Schmid).

1083-8791/$ – see front matter © 2014 American Society for Blood and Marrow Transplantation.
http://dx.doi.org/10.1016/j.bbmt.2014.05.002

evaluation of vascular remodeling regarding changes in wall thickness, lumen diameter, and passive mechanical properties, are lacking.

In our actual study, we aimed to characterize for the first time directly functional and structural alterations of mesenteric resistance arteries in an animal model of acute GVHD. Therefore, mesenteric arteries of mice that underwent allogeneic and syngeneic transplantation as well as untreated BALB/c were investigated 4 weeks after transplantation in a small vessel myograph for endothelium-dependent and -independent vasodilatory function, as well as mechanical properties. This principle is a very well–accepted method in cardiovascular research to directly characterize vascular function ex vivo [27]. After functional characterization, arteries were analyzed by electron microscopy for structural alterations.

MATERIALS AND METHODS

Experimental Bone Marrow Transplantation

Female C57BL/6N (H-2^b) and BALB/c (H-2^d) mice were purchased from Charles River Laboratories (Charles River, Sulzbach, Germany) and acclimatized in our animal facility for at least 1 week before starting the experiments. All animal experiments were approved by the local institutional animal committee of the University of Regensburg and were performed in accordance with German animal protection laws. Mice were between 11 and 12 weeks old at the time of BMT. They were housed in micro-isolator cages with autoclaved bedding and received autoclaved chow and water. Mice underwent transplantation as previously described [28]. On the day of BMT, BALB/c recipient mice received lethal total body irradiation with a total dose of 9 Gy, delivered in 1 fraction using a linear accelerator with 150 cGy/minute. After conditioning, the mice received 2.5×10^6 bone marrow cells and 2×10^6 splenocytes from either syngeneic (BALB/c, n = 5, synTx) or allogeneic (C57BL/6, n = 9, alloTx) donors. Untreated animals served as controls to detect possible effects of irradiation and transplantation procedures (n = 8, ctrl). Four animals that in the alloTx group died between day 6 and day 28 after BMT, whereas all animals that in synTx and ctrl groups survived the observation period of 4 weeks.

Clinical GVHD scores were assessed weekly by a scoring system incorporating 5 clinical parameters: weight loss, posture (hunching), mobility, fur texture, and skin integrity [29]. Each parameter was graded between 0 and 2 and the cumulative score for each mouse was calculated. Once an animal reached a cumulative score > 6.0, a weight loss of > 35%, or an absolute weight of < 13 g, it was sacrificed and counted as death due to transplantation-related mortality [29]. Blood pressure was assessed at week -1, +1, and +3 after transplantation by tail cuff method using an automated cuff inflator-pulse detection system (CODA2 Multi-Channel, Computerized, EMKA Technologies, Paris, France). In week +4, the surviving 8 ctrl, 5 alloTx, and 5 synTx animals were sacrificed and the mesenteric vasculature was dissected for the preparation of small resistance arteries.

Myograph Study

The myograph study was performed according to well-established protocols in our laboratory [30,31]. In brief, for each animal, 1 second-order branch of the superior mesenteric artery was prepared and mounted on a pressurized myograph (111 P; Danish Myo Technology, Aarhus, Denmark). Arteries were perfused using oxygenated 37°C KREBS solution (95% O_2, 5% CO_2) pH 7.4–containing NaCl (118 mmol/L), KH_2PO_4 (1.18 mmol/L), KCl (4.7 mmol/L), $MgSO_4$ (1.18 mmol/L), $CaCl_2$ (2.5 mmol/L), D-Glucose (5.5 mmol/L), $NaHCO_3$ (25 mmol/L), and EDTA (.026 mmol/L). First, studies to characterize the active vasodilatory properties of the vessels were performed. After precontraction with norepinephrine (NE, 10^{-5} mol/L), endothelium-dependent vasodilation was assessed with acetylcholine (ACh) (10^{-10}-10^{-4} mol/L) and endothelium-independent vasodilation with the direct NO donor sodium nitroprusside (SNP) (10^{-9}-10^{-2} mol/L). For that purpose, at each concentration of the given agent, the vessels lumen diameter was determined after 5 minutes of incubation. Thereafter, vessels were equilibrated at a constant pressure of 45 mmHg, their media thickness and lumen diameter were measured, and parameters of vessel geometry were calculated (media/lumen ratio, cross-sectional area [CSA]). Then, myogenic tone was inactivated by calcium depletion through incubation with Ca^{2+}-free KREBS solution for 30 minutes. Intravascular pressure was raised from 3 to 10, 20, 30, and 40 mmHg, and then in 20 mmHg steps up to 140 mmHg, to assess passive mechanical properties (circumferential strain and stress). At each step, the pressure was maintained until a steady-state diameter was reached and changes in internal diameter and media thickness of vessels were assessed. All vessel measurements for vasodilatory and mechanical properties were performed at 3 points along the vessel with the use of a calibrated video system and the mean was calculated. Finally, vessels were prepared for electron microscopy.

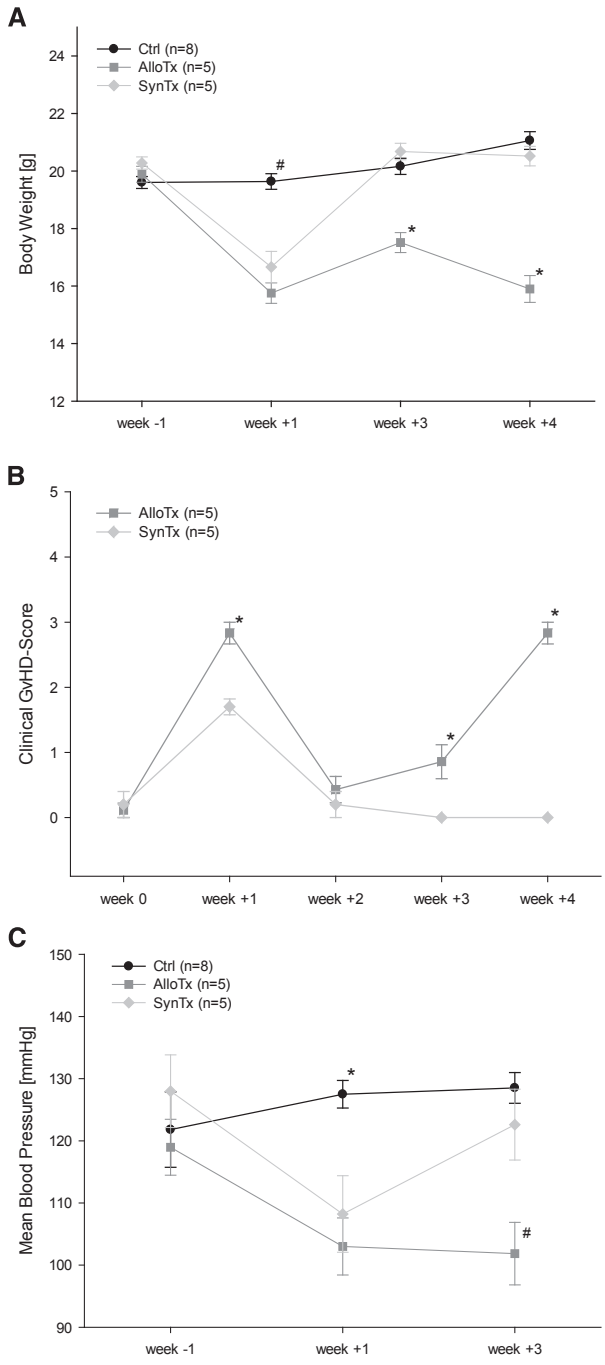

Figure 1. Biometric data of animals during the animal experiment. (A) Comparison of body weight between ctrl, alloTx, and synTx animals. Body weight significantly declines after allogeneic transplantation. One-way ANOVA for repeated measurements: $P < .001$. Post-hoc testing with Fisher LSD: $^*P < .001$ versus ctrl and synTx; $\#P < .001$ versus alloTx and synTx. (B) Clinical GVHD score of alloTx and synTx animals. The higher score after allogeneic transplantation indicates severe acute GVHD in these animals. Student *t*-test: $^*P < .05$ versus synTx. (C) Comparison of mean blood pressure between ctrls, alloTx, and synTx animals. Blood pressure significantly declines in alloTx animals after transplantation. One-way ANOVA for repeated measurements: $P < .001$. Post-hoc testing with Fisher LSD: * < .005 versus alloTx and synTx; # <.007 versus ctrl and synTx.

Expression of Endothelial and Inducible Nitric Oxide Synthase

The expression of endothelial (eNOS) and inducible nitric oxide (NO)–synthase (iNOS) in the small arteries was measured using a real-time RT-PCR as described previously [31]. In brief, mesenteric arteries of the second branch were collected and total RNA was extracted using RNeasy kit (Quiagen, Hilden, Germany), according to the instructions of the manufacturer. For first-strand cDNA synthesis, 1 μg total RNA was reverse transcribed with 1U MMLV Reverse Transcriptase, 1 μg Random Primer, 1 mM deoxynucleotide triphosphate mixture, 1 μL recombinant RNasin ribonuclease inhibitor, and transcription buffer with 5 mM $MgCl_2$ in a final volume of 10 μL (all from Promega, Mannheim, Germany). The reaction mixture was incubated at 37°C for 60 minutes, followed by heat inactivation of the enzyme at 95°C for 5 minutes. After cooling on ice for 5 minutes, the cDNA was stored at −20°C. In parallel, 1 μg total RNA was processed without reverse transcription to control for contamination with genomic DNA. Real-time RT-PCR detection of eNOS and iNOS was carried out using the ABIPrism 7900 TaqMan (Applied Biosystems, Foster City, CA). Beta-actin was used as housekeeping gene for normalization. Designed primers for beta-actin, eNOS, and iNOS were purchased from MWG Operon (Ebersberg, Germany). For each animal, measurements were carried out in triplicates and the mean was calculated.

Electron Microscopy

As described previously [32], vascular samples were fixed in buffered Karnovsky solution, postfixed in 1% osmium tetroxide, dehydrated in graded ethanols, and embedded in the EmBed-812 epoxy resin (all reagents from Science Services, Munich, Germany). Semithin (.8 μm) sections were cut and stained with toluidine blue/basic fuchsin. The whole vessel circumference was screened, areas of interest were selected, and the resin block was trimmed for further sectioning. Ultrathin (80 nm) sections were cut with a diamond knife on a Reichert Ultracut-S ultramicrotome (Leica, Vienna, Austria) and double contrasted with aqueous 2% uranyl acetate and lead citrate solutions. The sections were examined with a LEO912AB transmission electron microscope (Zeiss, Oberkochen, Germany) operating at 80 kilovolt in zero-loss mode. Images were documented (TIFF-format, calibrated for distance measurements) with a side-entry mounted 2000 × 2000 pixel digital camera. The electron microscopic examination included sections from 3 ctrl, 4 alloTx, and 3 synTx animals.

Data Analysis

For all biometric animal data (Figure 1) and property data (Table 1) of mesenteric arteries, means of every measurement for ctrl, alloTx, and synTx animals were calculated. Groups were compared using 1-way ANOVA (Fisher LSD as post-hoc test) or Student t-test as appropriate. The vessel vasodilation (Figures 2, 3) was calculated as percentage after a maximal precontraction with 10^{-5} mol/L norepinephrine using the following formula: vasodilation (%) = $(d_x\text{-}d_{NE})/(d_R\text{-}d_{NE}) \times 100$. Thereby, d_x is the actual measured diameter at a given concentration of ACh or SNP. d_{NE} is the diameter under precontraction with norepinephrine, and d_R is the resting diameter of the vessel. The curves created from these calculations were compared using 2-way ANOVA for repeated measurements with Holm-Sidak method as post-hoc test. The CSA of the media was calculated as $(\pi/4)(d_e^2\text{-}d_i^2)$ with d_e as external vessel diameter and d_i as lumen diameter of the vessel at 45 mmHg intraluminal pressure (Table 1). Circumferential strain (Figure 4) was calculated as $\varepsilon = (d_i\text{-}d_0)/d_0$, where d_i was the observed lumen diameter at a given intraluminal pressure and d_0 was the original diameter measured at 3 mmHg, respectively. Circumferential stress (Figure 5) was calculated as $\sigma = (pd_i)/(2m)$ according to Laplace's law with p being the intraluminal pressure, d_i the luminal diameter, and m the media thickness. Strain and stress of the different groups were compared using 2-way ANOVA for repeated measurements (Holm-Sidak method as post-hoc test). The strain/stress relation (Figure 6) was fitted to an exponential curve (equation: $f[x] = ae^{bx}$) for each vessel, with b as the slope of each single curve. The means of every calculated slope for each group were compared with ANOVA on rank (Dunn's method as post-hoc test). One-way ANOVA (Fisher LSD as post-hoc test) was used to analyze eNOS expression and ANOVA on Rank (Dunn's method as post-hoc test) for iNOS expression (Figure 7). All data are shown as mean ± SEM. A P value of $< .05$ was considered as significant.

Table 1
Geometry of Mesenteric Arteries at 45 mmHg of Intraluminal Pressure

Parameters	Ctrl (n = 8)	AlloTx (n = 5)	SynTx (n = 5)	*P* Value*
Media thickness, μm	11.0 ± .2	10.5 ± .1	11.2 ± .6	.37
Lumen diameter, μm	197.0 ± 7.4	217.7 ± 17.1	221.8 ± 18.4	.35
Media/lumen ratio	5.6 ± .2	4.9 ± .4	5.1 ± .3	.26
CSA, μm^2	7174 ± 293	7538 ± 598	8320 ± 1007	.41

* *P* values for 1-way ANOVA.

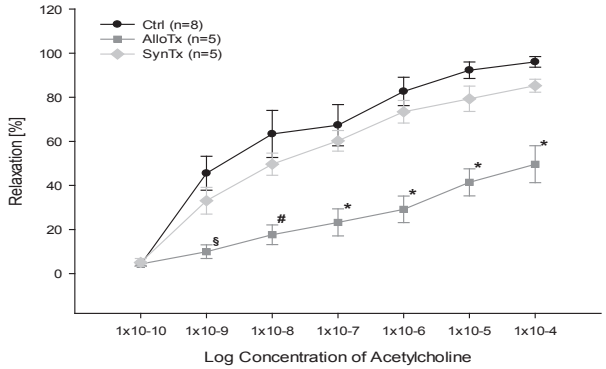

Figure 2. Endothelium-dependent vasodilatory response of mesenteric resistance arteries to increasing concentrations of acetylcholine (Ach). Vasodilatory response to ACh is diminished after allogeneic transplantation indicating endothelial dysfunction. Two-way ANOVA for repeated measurements: $P < .001$. Post-hoc testing with Holm-Sidak: *$P < .0001$ versus ctrl and synTx, #$P < .001$ versus ctrl and $P = .003$ versus synTx, §$P < .001$ versus ctrl and $P = .031$ versus synTx.

RESULTS

Body Weight, Clinical GVHD Score, and Blood Pressure

Figure 1 depicts the biometric animal data during the course of the animal experiment. At the beginning of the experiment, mice in each group weighed about 20 g. In ctrl animals, body weight slightly increased during the following weeks. In the first week after BMT, body weight clearly declined in both groups and recovered only in the syngeneic group, up to the level of control animals, until week +4. AlloTx animals, however, failed to recover body weight, resulting in a significant lower weight than in the control and synTx group in week +4. As expected, alloTx animals showed clinical signs of acute GVHD, objectified by the GVHD score. In contrast, synTx animals had no signs of GVHD in week +4. Systolic, diastolic, and mean blood pressure were similar in all groups at the start of the experiment and were stable in

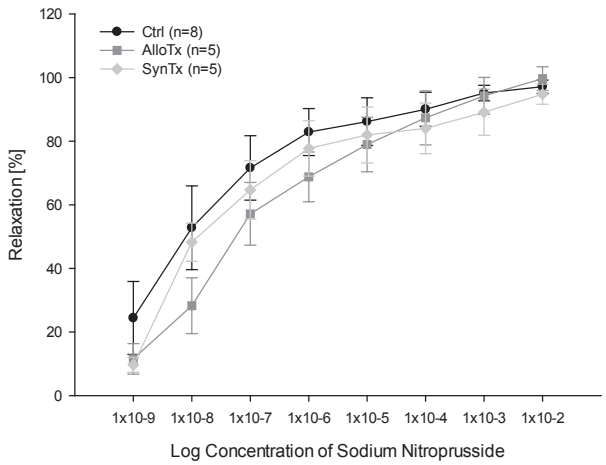

Figure 3. Endothelium-independent vasodilatory response of mesenteric resistance arteries to increasing concentrations of sodium nitroprusside. Vasodilatory response to sodium nitroprusside is unaffected after allogeneic or syngeneic transplantation. Two-way ANOVA for repeated measurements: $P = .33$.

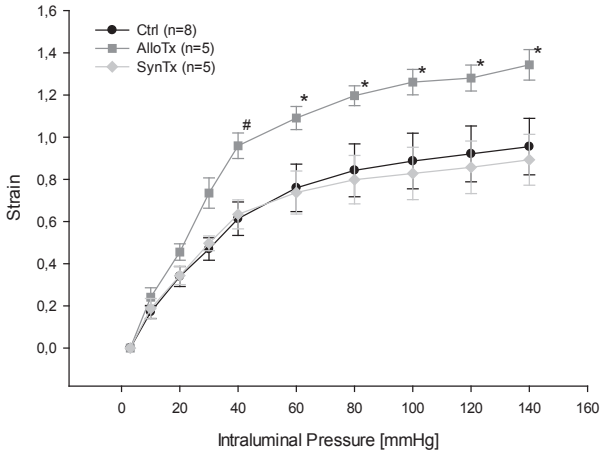

Figure 4. Strain as passive mechanical property of mesenteric arteries. Vessels exhibit a significant increased strain after allogeneic transplantation. Two-way ANOVA for repeated measurements: $P < .001$. Post-hoc testing with Holm-Sidak: $^{*}P < .05$ versus ctrl and synTx; $\#P < .05$ versus synTx.

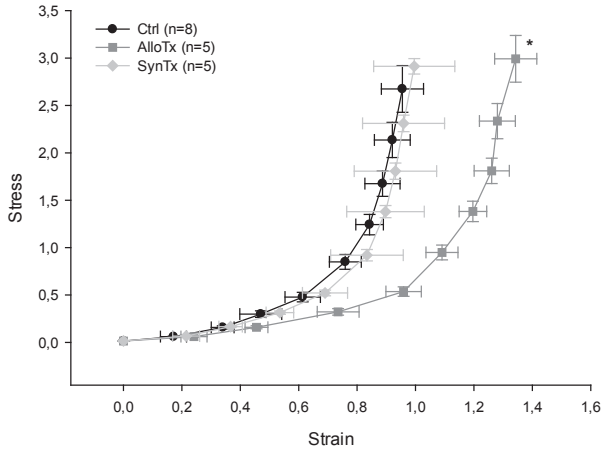

Figure 6. Strain/stress relationship as mechanical property of mesenteric arteries. Vessels after allogeneic transplantation show a right shift of their strain/stress relationship as an expression of an increased compliance at the same wall tension. Slope of strain/stress relation: ctrl 5.4 ± .7, alloTx 3.4 ± .03, and synTx 5.7 ± .9. ANOVA on rank $P = .007$. Post-hoc testing with Dunn's method: $^{*}P < .05$ for alloTx versus ctrl and synTx.

the ctrl group during the whole experiment. In the week after transplantation, blood pressure declined but soon regained the initial level in the synTx group. However, in the alloTx group, blood pressure did not rise again, resulting in significant lower systolic, diastolic, and mean blood pressure measurements in week +3 (Figure 1C exemplarily shows mean arterial blood pressure).

Vasodilatory Vessel Properties

We tested the vasodilatory response of mesenteric resistance arteries to increasing concentrations of ACh after a precontraction with norepinephrine (Figure 2). ACh stimulates the production of NO in endothelial cells, which leads to a relaxation of smooth muscle cells and, therefore, causes an endothelium-dependent vasodilation. We found significantly decreased vasodilation to ACh only in alloTx animals, indicating endothelial dysfunction after allogeneic BMT. In synTx animals, endothelial function did not differ significantly from the ctrl group. Maximum vasodilation reached at 10^{-4} mol/L of ACh was 49.7% ± 8.4%, 85.3 ± 2.9%, and 96.1 ± 2.4% in the alloTx, synTx, and ctrl group, respectively. Further, we examined the vasodilatory response to increasing concentrations of SNP after precontraction with norepinephrine (Figure 3). SNP is a direct NO donor, so the observed vasodilation depends only on smooth muscle cell function and not on endothelial function. Here, we found no differences between all investigated animal groups.

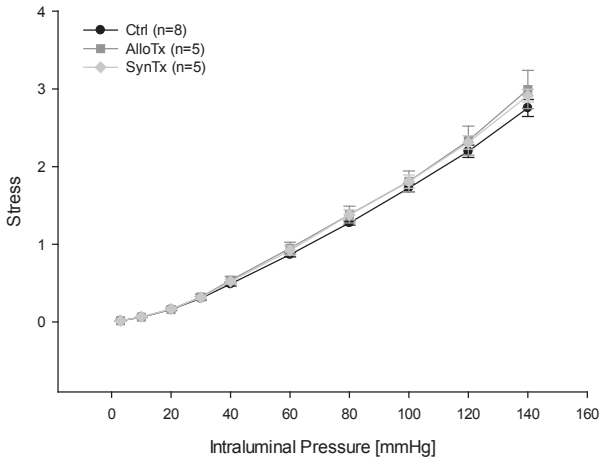

Figure 5. Stress as passive mechanical property of mesenteric arteries. Vessels stress is unchanged after allogeneic or syngeneic transplantation. Two-way ANOVA for repeated measurements: $P = .91$.

Morphological and Mechanical Vessel Properties

Table 1 shows the morphological data of the mesenteric arteries in the 3 investigated groups at 45 mmHg of intraluminal pressure. We could not detect any significant differences regarding media thickness, lumen diameter, media/lumen ratio, and CSA of the media. Circumferential strain (Figure 4) complies with the relative gain of lumen diameter with every increase in intraluminal pressure and, therefore, represents a measure of vessel compliance. The mesenteric arteries of alloTx mice showed a significantly increased strain

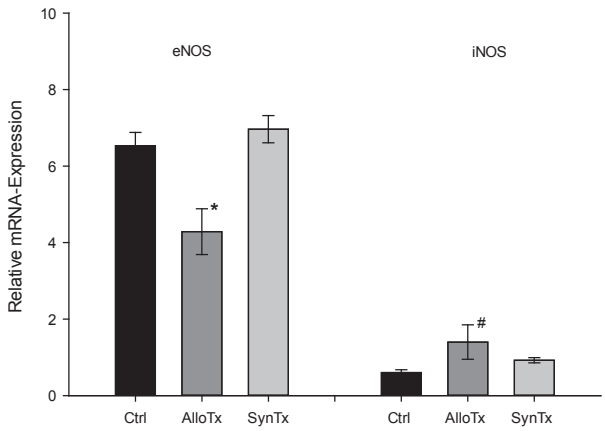

Figure 7. Relative expression of endothelial NO-synthase (eNOS) and inducible NO-synthase (iNOS) in mesenteric arteries. Expression of eNOS is decreased and iNOS is increased after allogeneic transplantation. N = 8 for ctrl, n = 5 for alloTx and synTx. One-way ANOVA for eNOS: $P = .003$. Post-hoc testing with Fisher LSD: $^{*}P = .003$ versus ctrl. and $P = .002$ versus synTx. ANOVA on Rank for iNOS: $P = .015$. Post-hoc testing with Dunn's method: $\#P < .05$ versus ctrl.

compared with ctrl and synTx animals. This means that vessels of alloTx animals were more distensible compared with ctrl and synTx animals. Circumferential stress (Figure 5) matches with the wall tension of vessels and was not significantly different between the different groups. This indicates that the higher vessel compliance in alloTx animals is independent of vessel geometry. This is further highlighted by the strain/stress relationship, which is depicted in Figure 6. The rightwards shift of the curve of alloTx animals indicates a higher distensibility, independent of vessel geometry, with a higher vessel strain at the same given stress. Accordingly, the comparison between the slopes of the strain/stress curves of each single vessel showed a significantly flatter curve for allogeneic recipients.

Expression of eNOS and iNOS

Figure 7 depicts the expression of eNOS and iNOS in the mesenteric arteries at mRNA level. ENOS expression in vessels of alloTx mice was significantly decreased in comparison with the ctrl and synTx groups. In contrast, iNOS expression was significantly upregulated compared with untreated animals.

Structural Vessel Changes

Electron microscopy was performed to reveal possible structural alterations after allogeneic BMT, which assert the observed changes in endothelial function and mechanical properties of the mesenteric arteries. The analysis in the control group illustrated, as expected, a normal vessel structure consisting of a plain endothelial cell layer at the luminal surface followed by the internal elastic lamina (tunica intima). The tunica media consists mainly of the smooth muscle cells and is outward bordered from the tunica adventitia by the lamina elastica externa. The investigation of the synTx group only showed discrete alterations compared with untreated animals. These changes affected the endothelial cells, where we could find an edema at some slices (not shown). However, after allogeneic transplantation, we could reveal very severe damage of all vessel layers (Figure 8). We found a perivascular accumulation of inflammatory cells in the tunica adventitia. Smooth muscle cells were degenerated and the tunica media showed localized liquid accumulations. The most severe damage was suffered in the endothelium. In large parts, endothelial cells were destroyed and detached from the lamina elastic interna. This resulted in great gaps between intact endothelial cells and a largely uncovered lamina elastica interna. In other parts, endothelial cells were edematous or had an increased pinocytotic activity. Furthermore, the lamina elastica interna and externa also had impressive abnormalities. Both layers could partly no longer be demarcated, as both were bulked or totally disintegrated.

DISCUSSION

To our knowledge, the present study is the first to describe, in detail, an involvement of mesenteric resistance arteries in an animal model of severe acute GVHD. As such, we proved the presence of endothelial dysfunction and increased vessel compliance after allogeneic BMT. These functional data correlate with a dysregulation of eNOS and iNOS at the mRNA level, as well as severe structural damages of the vessel wall, as visualized by electron microscopy. Therefore, our study further substantiates the hypothesis of a vascular form of GVHD.

Endothelial Dysfunction in GVHD

Our study was based on the investigation of functional properties of mesenteric resistance arteries in a pressurized myograph. This is an accepted and very well-established method in cardiovascular research [27]. We observed endothelium-dependent vasodilation in response to ACh, which was significantly reduced only in alloTx animals (Figure 2). At the same time, synTx animals did not exhibit endothelial dysfunction in comparison with untreated animals. Endothelium-independent vasodilation tested by the direct NO-donor SNP was unaffected after allogeneic or syngeneic transplantation, indicating a normal function of smooth muscle cells (Figure 3). Further, we analyzed the expression of eNOS and iNOS in the same mesenteric arteries. ENOS is mainly expressed in endothelial cells and activated by shear stress. It produces NO in a pulsatile calcium-dependent manner and has vasoprotective and antiatherosclerotic effects. ENOS-derived NO activates soluble guanylyl cyclase in smooth muscle cells and leads to vasodilation. In this context, endothelial dysfunction is characterized by the inability to produce adequate amounts of bioactive NO, which, among other factors, can be caused by a decreased expression of eNOS or eNOS uncoupling [33,34]. INOS can be activated in macrophages and many other cells in response to different inflammatory stimuli and produces a huge amount of NO calcium-independent. INOS-derived NO itself or peroxynitrite (formation of NO with O_2^-) are cytotoxic, not only for microbes and tumor cells, but also for healthy tissue, and can contribute to eNOS uncoupling and endothelial dysfunction [33,34]. Therefore, the downregulation of eNOS and upregulation of iNOS in the mesenteric arteries after allogeneic BMT (Figure 7) is able to explain endothelial dysfunction. The finding of increased iNOS activity is further substantiated by several studies showing excessively elevated NO levels in intestinal GVHD [35-41], whereas no data are available so far about eNOS expression in arteries of recipients with or without GVHD after allogeneic BMT. Up until now, endothelial dysfunction was only suggested indirectly by serum markers of endothelial function [22-26]. This makes our study the first to directly prove endothelial dysfunction, defined as a decreased vasodilatory response to ACh in GVHD.

Increased Vessel Compliance in GVHD

Further, we investigated mechanical vessel properties under no-flow conditions in the myograph. Thereby, possible flow-mediated changes in vessel diameters or the release of vasodilatory mediators like NO by shear stress can be mostly excluded. Besides, the vessels' own myogenic tone was inactivated by calcium depletion so that the observed changes in lumen diameter and wall thickness with increasing intraluminal pressure almost solely reflect passive vessel mechanics. Our finding of a greater gain of the vessel diameters with the stepwise increase of intraluminal pressure in alloTx animals with GVHD compared with synTx and ctrl animals means that the circumferential wall strain of vessels with GVHD is more pronounced (Figure 4). This is equivalent to a reduced arterial stiffness or increased vessel distensibility in GVHD. Such changes in passive mechanical vessel properties can be caused by geometry-dependent and -independent factors [42]. Because we could not find any sign for vascular remodeling or hypertrophy as ascertained by media thickness, lumen diameter, media/lumen ratio, and CSA of the media (Table 1), geometry-dependent alterations do not seem to be causative for the increased distensibility.

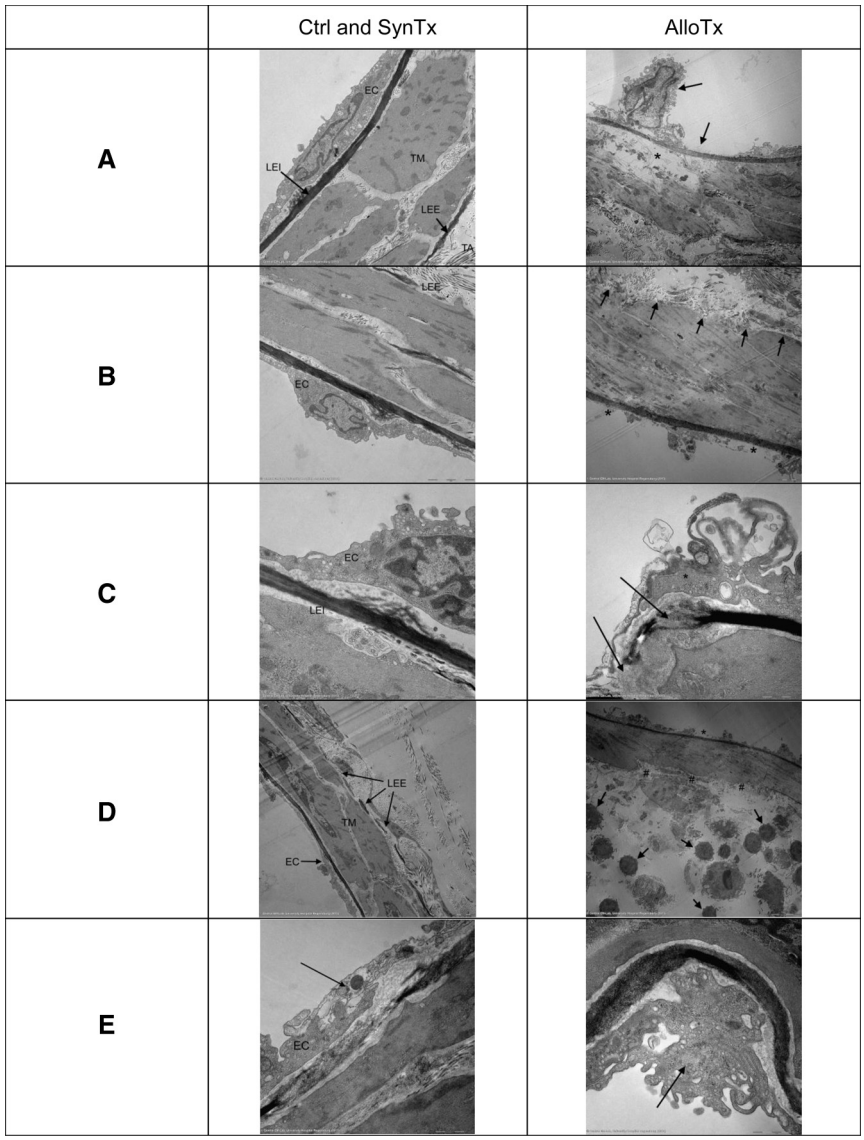

Figure 8. Electron microscopy of mesenteric arteries from ctrl and synTx animals in the left column and alloTx animals in the right column. (A) Normal vessel wall in untreated animals with an intact endothelial cell layer (EC), lamina elastica interna (LEI), tunica media (TM), lamina elastica externa (LEE) and tunica adventitia (TA). Original magnification × 10,000. In comparison, severe vessel wall damage in alloTx mice is shown. Endothelial cells are destroyed or detached from the LEI (→). Smooth muscle cells are degenerative, TM shows liquid accumulation (*). Original magnification × 5000. (B) SynTx animals show also a normal vessel wall with an intact EC and LEE. Original magnification × 10,000. In contrast, LEE is dissolved (→) and the LEI is uncovered (*) in alloTx mice. Original magnification × 5000. (C) Arteries of synTx animals show an intact LEI. Original magnification × 20,000. LEI is bulked (→) and endothelial cells are edematous (*) in alloTx mice. Original magnification × 20,000. (D) In synTx animals, no inflammatory cells can be found in the tunica adventitia. Original magnification × 5000. In contrast, perivascular accumulation of inflammatory cells in alloTx mice (→). Furthermore, the endothelium shows severe damage (detached endothelium *) and the lamina elastic externa is not definable over a distinct range (#). Original magnification × 1600. (E) Some endothelial cells in synTx animals show edema (→). Original magnification × 20,000. Intact endothelial cells in alloTx mice exhibit an increased pinocytotic activity (→). Original magnification × 20,000.

This was further supported by a similar circumferential wall tension in the 3 groups (Figure 5). In fact, the right shift of the strain/stress relationship clearly indicates geometry-independent reasons for the increased arterial compliance, because this means that at a given wall tension, the strain of the vessels in alloTx mice was significantly increased (Figure 6).

To our knowledge, our present study is the first to study directly the mechanical properties of mesenteric resistance arteries in acute GVHD. In chronic GVHD, a study in humans evaluated the compliance of the aorta via ultrasound [43]. In contrast to our study, they found an increased arterial stiffness in patients with disease duration of about 15 months. Arterial stiffness is an independent risk factor for cardiovascular events [44-47] and associated with different inflammatory diseases [48]. In this context, it is not surprising that in chronic GVHD, which is characterized by a chronic inflammatory process [49], arterial stiffness develops. However, the finding of reduced arterial stiffness in acute GVHD is new. So far, an increase in arterial compliance is, to our knowledge, only described in liver cirrhosis, where a hyperdynamic splanchnic circulation predominates [32,50-53]. Similarly, increased intestinal blood flow in the superior mesenteric artery and the bowel wall was detected in patients with acute GVHD by ultrasound [54]. This matches our findings, as the intestinal blood flow is regulated by the tone of the mesenteric resistance arteries. We see the decreased arterial blood pressure observed in patients as the clinical

correlate of the increased arterial compliance detected in our animals (Figure 1).

Structural Vessel Changes in GVHD

One of the mainstays of our study is that we could analyze the same arteries, from which we gathered the functional data in the myograph, for structural changes with electron microscopy. As far as we know, this has never been done in an animal model of GVHD before. Although vessels after syngeneic transplantation only showed discrete changes, such as endothelial cell edema, arteries after allogeneic transplantation exhibited very severe structural damage affecting the whole vessel wall. This is of interest because, so far, only an endothelium involvement was suggested in GVHD [5,9,10]. Besides, we could correlate all functional alterations in GVHD with structural findings. The endothelial dysfunction is very well explained by the destroyed and detached endothelium. Even the reduced expression of eNOS can be explained by the fewer endothelial cells as main source of eNOS expression. The exact mechanism of endothelial cell death remains unclear in our study. Some cells exhibit electron microscopic signs of apoptosis comparable with those described by Sho et al. [55], but in some others, necrosis is probable. As discussed below, we would expect apoptosis as the main mechanism, but necrosis induced by concomitant infections will certainly contribute to cell death in GVHD. However, further studies addressing the endothelial cell death in GVHD need to be done. As a correlate for the increased vessel compliance, we found bulked lamina elastica interna and externa, as well as the edema of the tunica media. As a source of the increased expression of iNOS, we considered the accumulation of inflammatory cells in the tunica adventitia. However, the described damage of smooth muscle cells seems not to be relevant, as the endothelium-independent vasodilation was not affected in GVHD.

Role of GVHD

In our study, allogeneic and syngeneic BMT were performed under the same conditions, including total body irradiation with 9 Gy and infusion of 2.5×10^6 bone marrow cells and 2×10^6 splenocytes. Of notice, animals received no conditioning chemotherapy. As anticipated, only alloTx mice developed a severe acute form of GVHD, which was confirmed by the clinical GVHD score and a continuous weight loss (Figure 1). This means that the observed functional and structural alterations in mesenteric arteries must be caused solely by GVHD and are independent of the irradiation, the transplantation procedure itself, or, in humans, usual conditioning chemotherapy. The pathophysiology of GVHD is characterized by a complex orchestra of different cellular effectors (mainly cytotoxic T lymphocytes and natural killer cells) and diverse cytokines (such as interferon γ, TNF, and NO) and finally results in apoptotic target tissue destruction [2]. Importantly, GVHD can cause endothelial cell apoptosis in different manners. It is known that T cells are able to induce endothelial apoptosis by the perforin/granzyme exocytosis and Fas/Fas ligand death pathway [56]. Also, interferon γ and TNF are able to destroy endothelial cells [57-62], an effect that is partly mediated by NO [63], which has, in high concentrations, cytotoxic effects [33,34]. Therefore, we hypothesize that the increased iNOS expression in our study in allogeneic transplant–recipient mice (Figure 7) is, among others, responsible for endothelial cell damage. In this context, therapeutic or prophylactic approaches to inhibit iNOS may be promising. However, the exact mechanisms underlying the vascular damage need to be further investigated.

CONCLUSION

In conclusion, our study provides further data to prove, and is the first to characterize, the involvement of the vasculature in GVHD. Our electron microscopic analysis of mesenteric arteries revealed severe damage of the whole vessel wall after allogeneic BMT. This correlates with functional alterations of the vessels in terms of endothelial dysfunction, which may be caused by a dysregulation of NO-synthases, and an increased compliance. Taken together, our study strongly supports the hypothesis of a self-contained vascular form of GVHD. Because endothelial dysfunction and mechanical vessel properties can also be measured noninvasively in humans by flow-mediated vasodilation and pulse-wave velocity, it would be of great interest if these results can be replicated in patients with GVHD. Further studies to understand the underlying mechanisms, especially for endothelial cell death, are now needed. As the contribution of vascular damage to tissue damage in GVHD seems possible, endothelium-protective treatments may be used to ameliorate systemic GVHD.

ACKNOWLEDGMENTS

We thank Gabriela Pietrzyk and Heiko Siegmund for excellent technical assistance.

Financial disclosure statement: The study was supported by a grant of the “Regensburger Forschungsförderung in der Medizin” (ReForMA) to P.M. Schmid.

Conflict of interest statement: There are no conflicts of interest to report.

REFERENCES

1. Choi S, Reddy P. Graft-versus-host disease. *Panminerva Med*. 2010;52:111-124.
2. Ferrara JL, Levine JE, Reddy P, Holler E. Graft-versus-host disease. *Lancet*. 2009;373:1550-1561.
3. Mastaglio S, Stanghellini MT, Bordignon C, et al. Progress and prospects: graft-versus-host disease. *Gene Ther*. 2010;17:1309-1317.
4. Biedermann BC, Sahner S, Gregor M, et al. Endothelial injury mediated by cytotoxic T lymphocytes and loss of microvessels in chronic graft versus host disease. *Lancet*. 2002;359:2078-2083.
5. Tichelli A, Gratwohl A. Vascular endothelium as 'novel' target of graft-versus-host disease. *Best Pract Res Clin Haematol*. 2008;21:139-148.
6. Padovan CS, Bise K, Hahn J, et al. Angiitis of the central nervous system after allogeneic bone marrow transplantation? *Stroke*. 1999;30:1651-1656.
7. Tichelli A, Rovo A, Gratwohl A. Late pulmonary, cardiovascular, and renal complications after hematopoietic stem cell transplantation and recommended screening practices. *Hematology Am Soc Hematol Educ Program*. 2008;125-133.
8. Holler E, Kolb HJ, Hiller E, et al. Microangiopathy in patients on cyclosporine prophylaxis who developed acute graft-versus-host disease after HLA-identical bone marrow transplantation. *Blood*. 1989;73:2018-2024.
9. Zhou H, Li Q, Zou P, You Y. Endothelial cells: a novel key player in immunoregulation in acute graft-versus-host disease? *Med Hypotheses*. 2009;72:567-569.
10. Biedermann BC. Vascular endothelium and graft-versus-host disease. *Best Pract Res Clin Haematol*. 2008;21:129-138.
11. Dumler JS, Beschorner WE, Farmer ER, et al. Endothelial-cell injury in cutaneous acute graft-versus-host disease. *Am J Pathol*. 1989;135:1097-1103.
12. Sviland L, Sale GE, Myerson D. Endothelial changes in cutaneous graft-versus-host disease: a comparison between HLA matched and mismatched recipients of bone marrow transplantation. *Bone Marrow Transplant*. 1991;7:35-38.
13. Yan Z, Zeng L, Jia L, et al. Increased numbers of circulating ECs are associated with systemic GVHD. *Int J Lab Hematol*. 2011;33:507-515.
14. Willemze AJ, Bakker AC, von dem Borne PA, et al. The effect of graft-versus-host disease on skin endothelial and epithelial cell chimerism in stem-cell transplant recipients. *Transplantation*. 2009;87:1096-1101.

15. Norton J, al-Saffar N, Sloane JP. Adhesion molecule expression in human hepatic graft-versus-host disease. *Bone Marrow Transplant*. 1992;10:153-156.
16. Sostak P, Reich P, Padovan CS, et al. Cerebral endothelial expression of adhesion molecules in mice with chronic graft-versus-host disease. *Stroke*. 2004;35:1158-1163.
17. Norton J, Sloane JP, al-Saffar N, Haskard DO. Vessel associated adhesion molecules in normal skin and acute graft-versus-host disease. *J Clin Pathol*. 1991;44:586-591.
18. Norton J, Sloane JP, al-Saffar N, Haskard DO. Expression of adhesion molecules in human intestinal graft-versus-host disease. *Clin Exp Immunol*. 1992;87:231-236.
19. Norton J, Sloane JP, Delia D, Greaves MF. Reciprocal expression of CD34 and cell adhesion molecule ELAM-1 on vascular endothelium in acute cutaneous graft-versus-host disease. *J Pathol*. 1993;170: 173-177.
20. Roy J, Platt JL, Weisdorf DJ. The immunopathology of upper gastrointestinal acute graft-versus-host disease. Lymphoid cells and endothelial adhesion molecules. *Transplantation*. 1993;55:572-578.
21. Matsuda Y, Hara J, Osugi Y, et al. Serum levels of soluble adhesion molecules in stem cell transplantation-related complications. *Bone Marrow Transplant*. 2001;27:977-982.
22. Kanamori H, Maruta A, Sasaki S, et al. Diagnostic value of hemostatic parameters in bone marrow transplant-associated thrombotic microangiopathy. *Bone Marrow Transplant*. 1998;21:705-709.
23. Nurnberger W, Michelmann I, Burdach S, Gobel U. Endothelial dysfunction after bone marrow transplantation: increase of soluble thrombomodulin and PAI-1 in patients with multiple transplant-related complications. *Ann Hematol*. 1998;76:61-65.
24. Salat C, Holler E, Kolb HJ, et al. Endothelial cell markers in bone marrow transplant recipients with and without acute graft-versus-host disease. *Bone Marrow Transplant*. 1997;19:909-914.
25. Testa S, Manna A, Porcellini A, et al. Increased plasma level of vascular endothelial glycoprotein thrombomodulin as an early indicator of endothelial damage in bone marrow transplantation. *Bone Marrow Transplant*. 1996;18:383-388.
26. Matsumoto T. Hemostatic abnormalities and changes following bone marrow transplantation. *Clin Appl Thromb Hemost*. 2004;10:341-350.
27. Schiffrin EL, Hayoz D. How to assess vascular remodelling in small and medium-sized muscular arteries in humans. *J Hypertens*. 1997;15: 571-584.
28. Bouazzaoui A, Spacenko E, Mueller G, et al. Steroid treatment alters adhesion molecule and chemokine expression in experimental acute graft-vs.-host disease of the intestinal tract. *Exp Hematol*. 2011;39: 238-249.e1.
29. Cooke KR, Kobzik L, Martin TR, et al. An experimental model of idiopathic pneumonia syndrome after bone marrow transplantation: I. The roles of minor H antigens and endotoxin. *Blood*. 1996;88:3230-3239.
30. Resch M, Schmid P, Amann K, et al. Eplerenone prevents salt-induced vascular stiffness in Zucker diabetic fatty rats: a preliminary report. *Cardiovasc Diabetol*. 2011;10:94.
31. Schmid PM, Resch M, Steege A, et al. Globular and full-length adiponectin induce NO-dependent vasodilation in resistance arteries of Zucker lean but not Zucker diabetic fatty rats. *Am J Hypertens*. 2011;24: 270-277.
32. Resch M, Wiest R, Moleda L, et al. Alterations in mechanical properties of mesenteric resistance arteries in experimental portal hypertension. *Am J Physiol Gastrointest Liver Physiol*. 2009;297:G849-G857.
33. Thomas DD, Ridnour LA, Isenberg JS, et al. The chemical biology of nitric oxide: implications in cellular signaling. *Free Radic Biol Med*. 2008;45:18-31.
34. Forstermann U, Sessa WC. Nitric oxide synthases: regulation and function. *Eur Heart J*. 2012;33:829-837. 837a-837d.
35. Weiss G, Schwaighofer H, Herold M, et al. Nitric oxide formation as predictive parameter for acute graft-versus-host disease after human allogeneic bone marrow transplantation. *Transplantation*. 1995;60: 1239-1244.
36. Vora A, Monaghan J, Nuttall P, Crowther D. Cytokine-mediated nitric oxide release—a common cytotoxic pathway in host-versus-graft and graft-versus-host reactions? *Bone Marrow Transplant*. 1997;20: 385-389.
37. Nestel FP, Greene RN, Kichian K, et al. Activation of macrophage cytostatic effector mechanisms during acute graft-versus-host disease: release of intracellular iron and nitric oxide-mediated cytostasis. *Blood*. 2000;96:1836-1843.
38. Langrehr JM, Murase N, Markus PM, et al. Nitric oxide production in host-versus-graft and graft-versus-host reactions in the rat. *J Clin Invest*. 1992;90:679-683.
39. Langrehr JM, Muller AR, Bergonia HA, et al. Detection of nitric oxide by electron paramagnetic resonance spectroscopy during rejection and graft-versus-host disease after small-bowel transplantation in the rat. *Surgery*. 1992;112:395-401. discussion 401-402.
40. Ellison CA, Natuik SA, McIntosh AR, et al. The role of interferon-gamma, nitric oxide and lipopolysaccharide in intestinal graft-versus-host disease developing in F1-hybrid mice. *Immunology*. 2003;109:440-449.
41. Choi IC, Fung PC, Leung AY, et al. Plasma nitric oxide is associated with the occurrence of moderate to severe acute graft-versus-host disease in haemopoietic stem cell transplant recipients. *Haematologica*. 2001;86: 972-976.
42. Dobrin PB. Mechanical properties of arteries. *Physiol Rev*. 1978;58: 397-460.
43. Dogdu O, Kaya MG, Yarlioglues M, et al. Impaired aortic elastic properties in patients with chronic graft-versus-host disease. *Echocardiography*. 2011;28:1011-1018.
44. Laurent S, Alivon M, Beaussier H, Boutouyrie P. Aortic stiffness as a tissue biomarker for predicting future cardiovascular events in asymptomatic hypertensive subjects. *Ann Med*. 2012;44(Suppl 1): S93-S97.
45. Laurent S, Katsahian S, Fassot C, et al. Aortic stiffness is an independent predictor of fatal stroke in essential hypertension. *Stroke*. 2003;34: 1203-1206.
46. Laurent S, Boutouyrie P, Asmar R, et al. Aortic stiffness is an independent predictor of all-cause and cardiovascular mortality in hypertensive patients. *Hypertension*. 2001;37:1236-1241.
47. Stefanadis C, Dernellis J, Tsiamis E, et al. Aortic stiffness as a risk factor for recurrent acute coronary events in patients with ischaemic heart disease. *Eur Heart J*. 2000;21:390-396.
48. Park S, Lakatta EG. Role of inflammation in the pathogenesis of arterial stiffness. *Yonsei Med J*. 2012;53:258-261.
49. Holler E. Cytokines, viruses, and graft-versus-host disease. *Curr Opin Hematol*. 2002;9:479-484.
50. Moller S, Gulberg V, Becker U, et al. Elevated arterial compliance in patients with cirrhosis is not related to arterial endothelin-1. *Scand J Gastroenterol*. 2002;37:1064-1069.
51. Henriksen JH, Gulberg V, Gerbes AL, et al. Increased arterial compliance in cirrhosis is related to decreased arterial C-type natriuretic peptide, but not to atrial natriuretic peptide. *Scand J Gastroenterol*. 2003;38: 559-564.
52. Henriksen JH, Moller S, Schifter S, Bendtsen F. Increased arterial compliance in decompensated cirrhosis. *J Hepatol*. 1999;31:712-718.
53. Henriksen JH, Kiszka-Kanowitz M, Bendtsen F. Review article: volume expansion in patients with cirrhosis. *Aliment Pharmacol Ther*. 2002; 16(Suppl 5):12-23.
54. Klein SA, Martin H, Schreiber-Dietrich D, et al. A new approach to evaluating intestinal acute graft-versus-host disease by transabdominal sonography and colour Doppler imaging. *Br J Haematol*. 2001;115:929-934.
55. Sho E, Sho M, Singh TM, et al. Blood flow decrease induces apoptosis of endothelial cells in previously dilated arteries resulting from chronic high blood flow. *Arterioscler Thromb Vasc Biol*. 2001;21:1139-1145.
56. Krupnick AS, Kreisel D, Popma SH, et al. Mechanism of T cell-mediated endothelial apoptosis. *Transplantation*. 2002;74:871-876.
57. Molostvov G, Morris A, Rose P, Basu S. Interaction of cytokines and growth factor in the regulation of verotoxin-induced apoptosis in cultured human endothelial cells. *Br J Haematol*. 2001;113:891-897.
58. Li JH, Kluger MS, Madge LA, et al. Interferon-gamma augments CD95(APO-1/Fas) and pro-caspase-8 expression and sensitizes human vascular endothelial cells to CD95-mediated apoptosis. *Am J Pathol*. 2002;161:1485-1495.
59. Pammer J, Weninger W, Ban J, et al. The cell death regulatory protein bak is expressed in endothelial cells in inflamed tissues and Is induced by IFN-gamma in vitro. *Biochem Biophys Res Commun*. 1999;264: 139-143.
60. Wang JH, Redmond HP, Watson RW, et al. Involvement of tyrosine protein kinase in IFN-gamma-induced human endothelial cell apoptosis. *Shock*. 1999;11:311-318.
61. Messmer UK, Briner VA, Pfeilschifter J. Basic fibroblast growth factor selectively enhances TNF-alpha-induced apoptotic cell death in glomerular endothelial cells: effects on apoptotic signaling pathways. *J Am Soc Nephrol*. 2000;11:2199-2211.
62. Xu C, Chang A, Hack BK, et al. TNF-mediated damage to glomerular endothelium is an important determinant of acute kidney injury in sepsis. *Kidney Int*. 2014;85:72-81.
63. Yamaoka J, Kabashima K, Kawanishi M, et al. Cytotoxicity of IFN-gamma and TNF-alpha for vascular endothelial cell is mediated by nitric oxide. *Biochem Biophys Res Commun*. 2002;291:780-786.